

# Accumulation of chromium metastable atoms into an Optical Trap

R. Chicireanu, Q. Beaufils, A. Pouderos, B. Laburthe-Tolra, E. Maréchal, L. Vernac, J.-C. Keller, and O. Gorceix

Laboratoire de Physique des Lasers, CNRS UMR 7538, Université Paris 13, 99 Avenue J.-B. Clément, 93430 Villetaneuse, France

**Abstract.** We report the fast accumulation of a large number of metastable  $^{52}\text{Cr}$  atoms in a mixed trap, formed by the superposition of a strongly confining optical trap and a quadrupolar magnetic trap. The steady state is reached after about 400 ms, providing a cloud of more than one million metastable atoms at a temperature of about  $100\ \mu\text{K}$ , with a peak density of  $10^{18}\ \text{atoms.m}^{-3}$ . We have optimized the loading procedure, and measured the light shift of the  $^5\text{D}_4$  state by analyzing how the trapped atoms respond to a parametric excitation. We compare this result to a theoretical evaluation based on the available spectroscopic data for chromium atoms.

**PACS.** 32.80.Pj Optical Cooling of atoms; trapping – 32.10.Dk Electric and magnetic moments, polarizability – 42.50.Vk Mechanical effects of light on atoms, molecules, electrons, and ions

## 1 Introduction

Optical dipole traps have proved to be an important tool to reach quantum degeneracy for a sample of neutral atoms since the first realization of Bose Einstein Condensates (BEC) by all optical means in 2001 [1]. It took for example a crucial part in the successful condensation of Cesium [2], and Chromium [3], for which high inelastic collision rates have prevented to achieve BEC inside a magnetic trap [4]. It was also necessary to use an optical trap (OT) to reach BEC with Ytterbium atoms, which have no magnetic moment ( $J=0$ ) in the ground state [5].

To reach BEC by evaporative cooling in a dipole trap, it is first necessary to load a tightly confining OT with typically a few million atoms. Given the available laser powers, such traps are very small, and it is hard to load them from large volume Magneto Optical Traps (MOT) or Magnetic Traps (MT). In the case of Cr, large light-assisted inelastic losses [6,7] make it particularly difficult to load an OT directly from a MOT. However, Cr atoms have a high magnetic moment, not only in the  $^7\text{S}_3$  ground state ( $6\ \mu_B$ , which makes Cr an interesting element to explore dipolar effects in quantum degenerate gases [8]), but as well in the metastable D states. This latter property allows continuous accumulation of a large number of cold metastable  $^{52}\text{Cr}$  atoms from a MOT into a MT [7, 9]: the atoms are optically pumped to the  $^5\text{D}_4$  and  $^5\text{D}_3$  metastable states by the cooling lasers (see Fig. 1), and remain trapped in the quadrupolar MT formed by the MOT coils. From this starting point, the successful strategy followed to reach quantum degeneracy for Cr [10] has been to accumulate the atoms in a Ioffe-Pritchard type elongated MT, compress this trap and perform Doppler

cooling in it after repumping to the ground state, load a single axis OT from this MT after some RF evaporative cooling, transfer the atoms into a crossed OT, and finally evaporatively cool them in the crossed OT by decreasing the laser power.

In this article we demonstrate that in 400 ms, more than one million metastable Cr atoms can be directly accumulated in the OT created by an intense laser beam crossing the MOT. After this accumulation, we repump the atoms back to the  $^7\text{S}_3$  ground state, switch the MOT magnetic gradient off, and optically pump the atoms to the absolute ground state  $|^7\text{S}_3, M_J = -3\rangle$  with a laser beam resonant with the 427.6 nm optical line (see Fig. 1). Our results may thus provide a new strategy to produce quantum degenerate gases of Cr atoms at a higher repetition rate, which may also be relevant for other atoms with metastable states, such as Sr, Er, or Yb.

Moreover, this article is to our knowledge the first to report the optical trapping of neutral atoms in a metastable state. Even if the optical trapping process is similar for metastable states and for the ground state, the measurement of the OT depth in the D state provides information on how this state couples to the other levels of the complicated electronic structure of Cr, and can yield in particular a determination of the polarizability of this state.

The paper is organized as follows. We first describe the experimental setup and characterize the OT. We then present our experimental results, which are the study of the loading of the OT, and the parametric excitation spectra of the OT loaded by atoms in the metastable  $^5\text{D}_4$  state. To take into account the trap anharmonicity, we perform 3D Monte Carlo simulations described in section 4. We thus deduce the light shifts for the  $^5\text{D}_4$  and the  $^7\text{S}_3$  states.

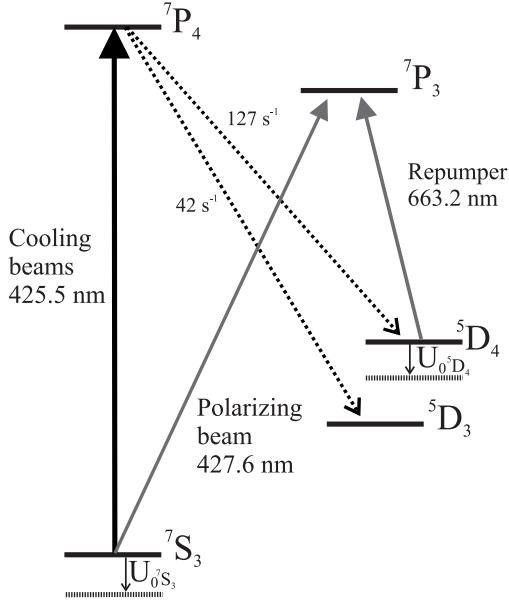


**Fig. 1.**  $^{52}\text{Cr}$  atomic levels relevant for the study, and optical lines used to cool, trap, repump or spin polarize the atoms. From the excited  $7P_4$  state the atoms decay to metastable D states at the indicated rates. The AC stark shifts induced by the trapping IR laser as mentioned in the text are shown.

Finally, we calculate the light shifts of the different Zeeman sublevels of the states of interest, using the spectroscopic data available for the optical transitions of Cr, and we conclude with a comparison with our measurements.

## 2 Realization of the optical trap

### 2.1 Experimental setup

The experiment starts with the production of a Cr atom beam from an oven heated at 1500 Celsius. The atoms are then decelerated as they travel through a one-meter-long Zeeman Slower (ZS), and they are trapped in a standard MOT. We typically obtain a Gaussian-shape cloud with a  $1/e$  radius of  $100\ \mu\text{m}$ , containing up to  $5 \times 10^6$   $^{52}\text{Cr}$  atoms at a temperature of  $100\ \mu\text{K}$  [7].

In previous works, we accumulated metastable D states atoms in the MT created by the MOT coils [7,11]. Here we study the loading of metastable atoms into the OT created by an horizontal laser beam focused at the MOT and MT center. This laser is a commercial 1075 nm 50 W Ytterbium fiber laser. After an optical isolator and some optical beam shaping to focus the laser in an Acousto Optic Modulator (AOM) and re-collimate it, we have up to 35 W available for atom trapping. We focus the laser at the MOT position with a plano convex lens of focal length  $f_{IR}$ . A weak part of the IR laser transmitted through a back-side-polished dielectric mirror is sent to a lens identical to the one producing the OT, so that we can measure parameters very close to the ones of the laser beam focused in the vacuum chamber. We obtained a waist of  $55(41) \pm 5$

$\mu\text{m}$ , and a Rayleigh length of  $5.5(3) \pm .5\text{ mm}$  with  $f_{IR}=20$  (respectively 15) cm.

In order to characterize the OT, we capture images of the atomic cloud using a standard absorption technique. The  $100\ \mu\text{s}$  imaging beam pulse is resonant with the  $7S_3 \rightarrow 7P_4$  transition ( $\lambda=425.5\text{ nm}$ ,  $I_{sat} = 8\text{ mW}\cdot\text{cm}^{-2}$ ), has an intensity of  $0.08 I_{sat}$ , and is circularly polarized. Its propagation axis lies in the horizontal plane, and is almost orthogonal to the ZS axis (see Fig. 2). It makes an angle  $\alpha = 7^\circ$  with the IR beam, which allows us to monitor the expansion of the cloud along the weak trapping  $z'$  axis of the OT.

Before taking an image, the atoms are repumped to the  $7S_3$  ground state, via the  $5D_4 \rightarrow 7P_3$  transition at 663.2 nm. For that purpose, we use a commercial monomode extended cavity diode laser. A 2 mW-power and 5 ms long pulse is sufficient to repump all the  $5D_4$  metastable atoms back in the ground state. An other diode running at 654 nm can repump the atoms in the  $5D_3$  state, so that we can monitor the accumulation of both metastable states in the OT. However in this paper we will concentrate on the  $5D_4$  state.

Then, a magnetic field of 2.8 Gauss is applied along  $z$ , and a  $50\ \mu\text{s}$  pulse at 427.6 nm, having an intensity of  $0.5 I_{sat}$  and the same circular polarization than the imaging beam, polarizes the atoms. Therefore during the imaging pulse the atoms cycle between the fully stretched  $|7S_3, M_J = -3\rangle \rightarrow |7P_4, M_J = -4\rangle$  Zeeman sublevels and the average absorption cross section  $\sigma_{opt}$  can be set to  $3\lambda^2/2\pi$  ( $\lambda = 425.5\text{ nm}$ ).

### 2.2 Characterization of the dipole trap

The atomic cloud center is conjugated on the CCD chip plane by a 1:1 imaging system. We will deal with two bases:  $(x, y, z)$  is used to describe the images, and  $(x', y, z')$  are the natural coordinates of the OT (see Fig. 2). The angle between  $z$  (the imaging beam axis) and  $z'$  (the weak trapping axis of the OT), or between  $x$  and  $x'$  (one of the strong trapping axis of the OT), is  $\alpha$ . We note  $y$  the vertical axis, which is therefore the other strong trapping axis of the OT.

From absorption images we obtain the Optical Depth,  $OD(x, y)$ , which is linked to the atomic density  $n(x, y, z)$  via:

$$OD(x, y) = \int_{-\infty}^{+\infty} \sigma_{opt} n(x, y, z) dz \quad (1)$$

Since the total number of atoms  $N_{at}$  in the trap is proportional to the total integral of  $OD(x, y)$  as given in eq. (1), we deduce its value from:

$$N_{at} = \frac{1}{\sigma_{opt}} \int_{-\infty}^{+\infty} \int_{-\infty}^{+\infty} OD(x, y) dx dy \quad (2)$$

To evaluate the integral in eq. (2), we first perform a numerical integration along  $x$  of  $OD(x, y)$ . The function ob-

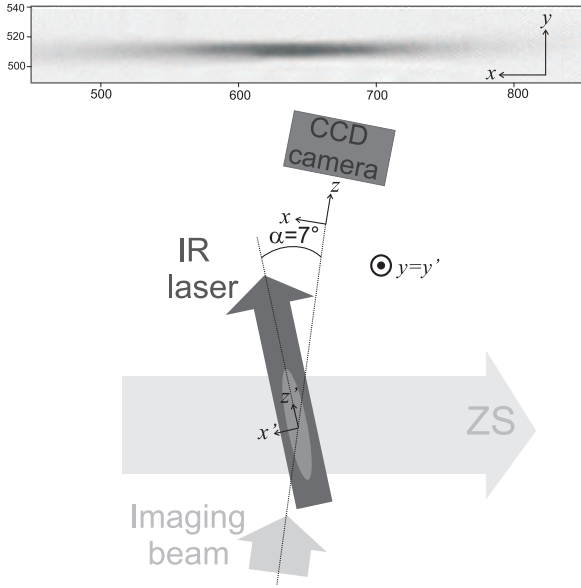


**Fig. 2.** Bottom: schematic of the imaging system. ZS stands for the Zeeman Slower beam. The imaging beam is partially absorbed by the atoms in the OT created by the IR laser, and passes through a 1:1 imaging system (not shown) before reaching the CCD camera chip. The axis of the two bases introduced in the text are shown. Top: Optical Depth along  $z$  after 400 ms of accumulation. The expansion along the  $x$  axis occurs during the switch-off time of the MOT coils B field. The size of the pixels is  $6.5 \mu\text{m}$ .

tained can be very well fitted by a Gaussian, and from the fit parameters we deduce the value of the integral.

To obtain the peak density  $n_0$  from  $OD$  measurements, one needs information on the atomic density distribution. The OT has a cylindrical revolution symmetry around its weak axis, and the density dependence on  $y$  is decoupled from the ones on  $x$  and  $z$ :  $n(x, y, z) = n(y)f(x, z)$ . A cut of  $OD(x, y)$  along  $y$  gives therefore the density distribution  $n(y) = n(x')$ . This distribution is well fitted by a Gaussian, with a  $1/e^2$  radius,  $W_t$ , equal to 50 (36)  $\mu\text{m}$  for  $f_{IR}=20$  (respectively 15) cm. In addition, if the width of the density along the weak axis  $z'$ ,  $\sigma_{z'}$ , is much larger than  $W_t$ , we have in the vicinity of the trap center:

$$n(x', y', z') \simeq n_0 e^{-\frac{2(x'^2 + y'^2)}{W_t^2}} \quad (3)$$

Using  $x' = x \cos(\alpha) - z \sin(\alpha)$ , we thus obtain:

$$n(x = 0, y = 0, z) = n_0 e^{-\frac{2 \sin(\alpha)^2 z^2}{W_t^2}} \quad (4)$$

By integrating eq. (4) we can therefore link the maximal value of the  $OD$ ,  $OD_{max}$ , to the peak density:

$$n_0 = \frac{OD_{max} \sin(\alpha)}{\sqrt{\frac{\pi}{2}} \sigma_{opt} W_t} \quad (5)$$

This equation is valid as long as the imaging beam path through the atomic cloud (along  $z'$ ) is short compared to

$\sigma_{z'}$ . This condition reads:  $\frac{W_t}{\tan(\alpha)} \ll \sigma_{z'}$ . Introducing the width of  $OD(x, y)$  along the  $x$  axis,  $\sigma_x = \sigma_{z'} \sin(\alpha)$ , we finally get the condition  $\sigma_x \gg W_t$ . Experimentally we measure  $\sigma_x \simeq 700 \mu\text{m}$ , so that  $n_0$  can be reliably deduced from eq. (5).

### 3 Experimental results

The experiments described in this section were obtained with  $f_{IR} = 15$  cm, except in subsection 3.3 where  $f_{IR} = 20$  cm.

#### 3.1 Accumulation of atoms in the OT

Here we turn to our first main experimental result, *ie* the accumulation of cold metastable Cr atoms in the OT.

We show how fast the loading proceeds on the top part of Figure 3. To increase the number of trapped atoms, we have retroreflected the IR laser beam, so that a total power of 70 W is sent to the atoms. The ZS, the MOT, and the IR laser are switched on for a given duration  $t$ . Due to eddy currents, it takes 20 ms for the magnetic fields to die away after the power supply driving the MOT coils is switched off. As a consequence, a 20 ms waiting time is necessary before taking an image of the OT. During this waiting time, the atom cloud has expanded along the  $x$  axis. For each loading time  $t$ , the total number of atoms is evaluated from eq. (2). A very short  $1/e$  loading time of typically  $\tau = 150$  ms is obtained.

From the image at  $t = 400$  ms, we deduce the following asymptotic numbers: a total atom number  $N_\infty = 1.2 \cdot 10^6$ , and a peak atomic density  $n_0 = 1.2 \cdot 10^{11} \text{ cm}^{-3}$ . We want to emphasize that the atomic density is much larger in the mixed trap (before the 20 ms expansion). Although it is difficult to extract the peak density from the in situ absorption images due to the complicated mixed trap geometry, we estimate that the longitudinal width is about 10 times smaller before expansion, so that the in situ density is about  $10^{12} \text{ cm}^{-3}$ .

In addition, we measured the temperature of the metastable atoms in the OT, by analyzing the free expansion along the vertical  $y$  axis after the OT has been switched off. When the IR power is at maximum, we obtain  $T_{OT} = (120 \pm 10) \mu\text{K}$ . In the bottom part of Figure 3, we see that while the number of trapped atoms increases with the trapping laser power, the parameter  $\eta$ , which is the ratio between the OT depth (average theoretical value, see eq. (11)) and the cloud temperature, remains almost constant ( $\eta \simeq 3$ ) for large IR power.

#### 3.2 Loading dynamics

To optimize the loading of the OT, we found that it is crucial that the IR laser remain on during the whole MOT loading process: we observe only little trapping if the dipole trap is turned on after the MOT beams have been switched

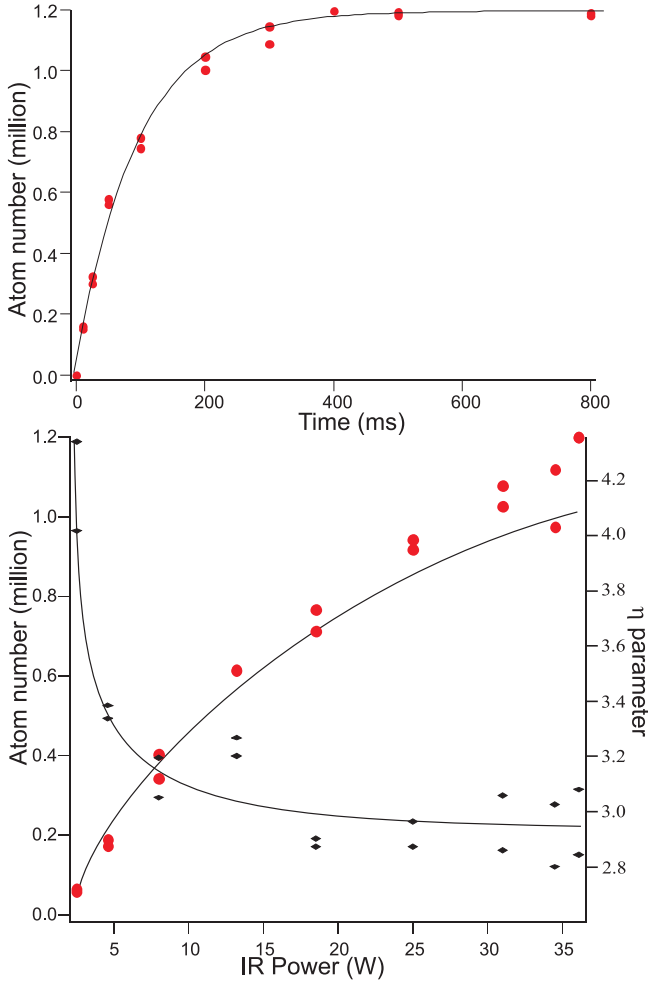


**Fig. 3.** Top: Loading sequence into the OT at the optimal IR beam focus position (see text), with the retroreflected beam, and at maximum laser power. The line is the result of an exponential fit. Bottom: dependance of the stationary number of atoms (circles) and of the  $\eta$  parameter (diamonds) - see text - with the trapping laser power, which is set by AOM control. The two lines are guides for the eye.

off. This indicates that the atoms are directly injected in the OT from the MOT, rather than from the MT. Indeed, an atom from the MOT traveling through the OT experiences both the acceleration due to the OT potential and the friction force of the MOT [12]. If friction is large enough, and if it gets optically pumped to the metastable states before it leaves the OT location, it will remain trapped in the OT.

To accurately discuss the loading physics and the alignment issue between the OT and the MOT, we show on Figure 4 the influence of the horizontal IR beam pointing on the stationary number of atoms in the OT,  $N_\infty$ ; there was no retroreflection of the IR beam in this experiment to simplify the analysis. We see that two optima are found for  $N_\infty$ . This shows that the optimal situation is reached when the IR beam is slightly off centered with respect to the MOT. Besides, we observed that the loading time is

longer when we set the IR beam at the optimal positions ( $x' = \pm 50 \mu\text{m}$ ,  $\tau = 240 \text{ ms}$ ), than if we set it at the local minimum position ( $x' = 0$ ,  $\tau_0 = 110 \text{ ms}$ ). As the loading time is set by the dominant loss rate, and as the inelastic loss rate between metastable states should be higher for a larger number of atoms, this rules out inelastic collisions between metastable states as the limiting factor for the loading of the OT. In addition, the loading factor at the optimal position is equal to the lifetime of the mixed trap at this position, which is measured when the MOT beams are turned off after accumulation. This rules out inelastic collisions with the MOT atoms as the limiting factor, which is quite different from what was observed for ground state OT loading from a MOT [13]. Finally, at low density, the  $1/e$  lifetime (9s) of the pure OT is much larger than the loading time, so that collisions with the background gas is not the limiting factor either.

We therefore think that the dominant source of losses when the OT is centered at  $B=0$  is a consequence of Majorana losses: spin flips in the vicinity of the zero B field position (which is as well the MOT center) are responsible for the dominant loss process. Indeed the high field seekers states are not trapped in the mixed trap, as they are expelled along the weak trapping axis of the OT by the MT gradient. When the IR beam is slightly off-centered, these losses decrease, which accounts for the larger loading time that we observe. At the same time the OT loading rate, proportional to the superposition with the MOT, decreases too, which leads to the experimental trade-off observed in Figure 4.

For a matter of fact, the observed loss rate per atom when the OT is centered at  $B=0$ ,  $1/\tau_0$ , is in qualitative agreement with a rough evaluation of the Majorana loss rate,  $\Gamma_{maj}$ . To perform this evaluation, we calculate the probability per second for an atom to cross the sphere of radius  $d$  where a spin flip is likely to happen, with  $d = \sqrt{\frac{h\bar{v}}{\mu b_0}}$  [14]. In this equality,  $\bar{v} = (k_B T/m)^{1/2}$  is the quadratic mean velocity along one axis in the mixed trap ( $k_B$  is the Boltzmann constant,  $m$  is the mass of the  $^{52}\text{Cr}$  atom,  $T$  is the temperature of the mixed trap);  $\mu$  is the magnetic moment of the  $^5D_4$  state ( $\mu = 6 \mu_B$ ), and  $b_0$  is the MT gradient. Along  $z'$ , the atom mostly feel the effect of the MT, and a simple geometric argument gives:

$$\Gamma_{maj} = a \frac{2}{\tau_{MT}} \left( \frac{d}{W_t} \right)^2 \quad (6)$$

where  $\tau_{MT}$  is the typical MT period along  $z'$ , and  $a$  is a numerical factor of the order of one (for example,  $a \simeq 3$  for a linear trap[14]). Using the experimental value for  $b_0$  ( $10 \text{ G.cm}^{-1}$ ),  $W_t$  ( $30 \mu\text{m}$ ), and  $T \simeq 100 \mu\text{K}$ , we obtain  $d = 4 \mu\text{m}$ ,  $\tau_{MT} = 30 \text{ ms}$ , and  $\Gamma_{maj}^{-1} = (800/a) \text{ ms}$ , while  $\tau_0 = 110 \text{ ms}$ .

### 3.3 Parametric excitation spectra

In this subsection, the IR laser is not retroreflected in order to reduce systematic effects, since the exact size and

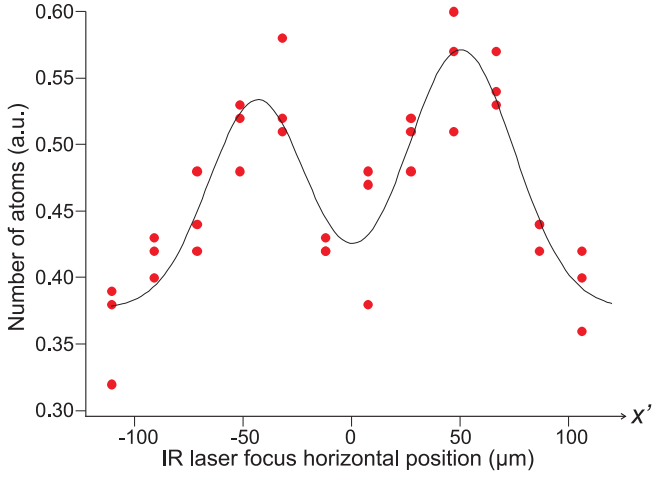


**Fig. 4.** Dependency of the steady number of atoms  $N_\infty$  with the IR laser focus position on the horizontal plane, with no retroreflection. If the IR beam is crossing the MOT center ( $x' = 0$ ), the atom number reaches a local minimum. The black line is a result of a fit with two Gaussians. The two peak centers are separated by 100  $\mu\text{m}$ .

shape of the retroreflected beam is hard to measure. As noted above,  $f_{IR} = 20$  cm. In this situation, the measured temperature at full power is  $70 \pm 10$   $\mu\text{K}$ , and the maximum number of atoms is 2 millions.

The measurement of an OT depth was performed by Friebe and coworkers a few years ago [15] by modulating the trap spring constant through the intensity of the trapping laser. Depending on the modulation frequency  $f_m$ , the atom cloud gets more or less heated, and atoms are driven out of the OT accordingly. The parametric excitation spectra correspond to the number of atoms remaining in the trap after a given modulation duration, as a function of  $f_m$ . The characteristics of these spectra reflect the trap potential shape.

We used the AOM controlling the trapping beam power to modulate the OT depth. The Radio Frequency power sent to the AOM is set at 80% of its maximal value, so that an average power of 29 W is sent to the atoms, and is modulated at a few kHz, with a peak to peak amplitude of 20%. To obtain the excitation spectrum of the  $^5\text{D}_4$  state, we first load the OT, and then modulate the IR laser intensity for 40 ms. After repumping the atoms back to the ground state, we measure  $N_{at}$ , as a function of  $f_m$ . An excitation spectrum of the metastable state is shown in Figure 5. We have also measured the excitation spectra of the  $^7\text{S}_3$  state, by first repumping the atoms, and then modulating the OT depth.

## 4 Simulation of the parametric excitation spectra

### 4.1 Classical 3D simulation of the parametric excitation process

Since the trap potential (approximately Gaussian shaped) is not harmonic, the parametric excitation spectra are both broadened and shifted compared to the ones which would be obtained in a purely harmonic trap, as noticed previously by other groups (see for example [16]). In order to deduce the light shifts of the levels of interest from the spectra described in subsection 3.3, we performed a 3D classical Monte Carlo simulation, which also allowed us to take into account the presence of the MT. The effect of both elastic and inelastic collisions are not taken into account in this analysis. We performed experimental parametric excitation for various excitation duration, and found no change in the experimental line shape, so that collisions can indeed be neglected.

The combined trap created by the MT and the OT is considered to be the sum of two potentials. First a Gaussian 2D potential (in the  $x'y'$  plane) corresponding to the OT strong trapping axis, with a depth  $U_0$  ( $U_0 < 0$ ) and a width  $W$ . Second, a linear 3D potential, corresponding to the quadrupolar magnetic field created by the MOT coils, described by the gradient  $b_0$ . During the simulation, the trapping laser intensity is modulated for a duration  $\Delta t$ , so that the atoms experience a time-dependent potential  $U(t)$  which reads as:

$$U(t) = U_0(1 + f(t))e^{-\frac{2r^2}{w^2}} + \overline{m_J} g_J \mu_B b_0 \sqrt{x'^2 + 4y'^2 + z'^2} \quad (7)$$

where  $r = \sqrt{x'^2 + y'^2}$ ,  $\overline{m_J}$  is the average magnetic quantum number ( $\overline{m_J} \simeq 2$ , see [11]), and  $f(t)$  is the function describing the time evolution of the trap depth.

In the Monte Carlo draw, the radial coordinate  $r$ , the longitudinal one  $z'$ , and the velocity  $V$  of the atoms, are selected according to a Gaussian probability distribution, with respective  $1/e^2$  width  $W_t$ ,  $\sigma_{z'}$ , and  $2(k_B T/m)^{1/2}$  ( $T$  is the temperature of the cloud). We evaluate the final values of the radial position ( $r_f$ ), velocity ( $V_f$ ), and the

energy  $E_f = \frac{1}{2}mV_f^2 + U_0e^{-\frac{2r_f^2}{w^2}}$ . We then evaluate the proportion of atoms remaining in the OT (which are those with  $E_f < 0$ ) for different values of the modulation frequency. We obtain the simulated parametric excitation spectra by normalizing to the result obtained when no modulation is applied.

The values of  $\Delta t$ ,  $W_t$ ,  $b_0$  and  $W$  are the experimental ones (40 ms, 50  $\mu\text{m}$ , 10  $\text{G}\cdot\text{cm}^{-1}$ , 55  $\mu\text{m}$ ).  $\sigma_{z'}$  is evaluated from images of the mixed trap ( $\sigma_{z'} \simeq 280$   $\mu\text{m}$ ). The function  $f(t)$  reproduces the experimental laser intensity modulation. The simulated spectra are quite insensitive to the temperature  $T$ . In the simulation of Figure 5,  $T = 120$   $\mu\text{K}$ .

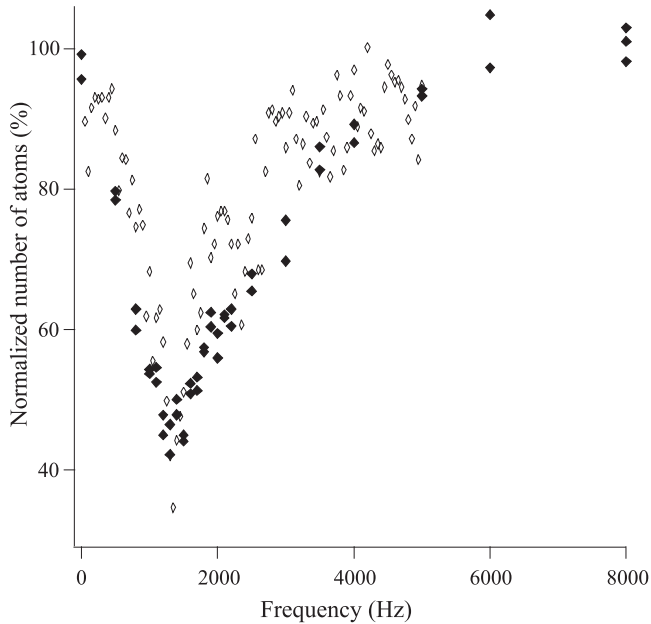


**Fig. 5.** Experimental and best adjusted simulated excitation spectra (open diamonds) for the  ${}^5D_4$  state. The normalized remaining number of atoms is plotted versus the trap modulation frequency.

## 4.2 Numerical results

We computed spectra for various value of  $U_0$ , using  $U_0$  as the only adjustable parameter. The simulated spectra are always narrower than the experimental ones, and we focused on the position of the central excitation frequency: we look for the value of  $U_0$  that gives a spectrum centered at the experimental resonance.

The experimental and the best central frequency adjusted theoretical spectra are shown for the  ${}^5D_4$  state in Figure 5. From this best adjustment, we deduce the following OT depth in MHz:  $U_0 {}^5D_4 = -(3.2 \pm 0.6 \pm 0.6)$  MHz. The first uncertainty of 20% is our estimate of the fit uncertainty. The second is a result of the 10% accuracy on the waist measurement. We have applied the same procedure to spectra obtained for atoms in the ground state (for which  $g_J = 2$ ), and obtained  $U_0 {}^7S_3 = -(3.8 \pm 0.7 \pm 0.7)$  MHz. As theoretical evaluations have already proved to be in good agreement with experimental values for the ground state light shifts [17], the comparison of  $U_0 {}^7S_3$  with calculations in the next section will allow us to test the validity of our procedure.

## 5 Theoretical evaluations of the light shifts and comparison with the experiment

We now turn to our theoretical estimates for the light shifts to compare with the experimental data.

When a given atomic level  $i$  having an energy  $\hbar\omega_i$  is coupled by a laser through dipolar electric transitions to other states  $n$  having energies  $\hbar\omega_n$ , its energy is shifted

due to the presence of the AC laser electric field. This light shift depends on  $I_L(r)$ , the local laser intensity, on  $\omega_{ni} = \omega_n - \omega_i$  and on  $\gamma_{ni}$  (respectively the angular frequency and the cycling rate of the transition between level  $i$  and level  $n$ ), and on  $\omega$  the laser angular frequency. In fact, the different Zeeman sublevels- corresponding to the magnetic quantum number  $M_{J_i}$  - are coupled differently to the excited states, and the light shift not only depends on the total angular momentum  $J_i$  but as well on  $M_{J_i}$ , and on the laser polarization. To simplify the discussion we take a nuclear spin equal to zero, which is the case for the bosonic  ${}^{52}\text{Cr}$  atom. The coupling rate between the sublevel  $(i, J_i, M_{J_i})$  and the excited state  $(n, J_n, M_{J_n})$  is given by a 3J coefficient, and one must distinguish between a coupling towards more energetic states ( $\omega_{ni} > 0$ ) or toward less energetic states ( $\omega_{ni} < 0$ ):

$$\gamma_{M_{J_i}, n} = \gamma_{ni} (2J_n + 1) \times C_{J_i, M_{J_i}, J_n, \text{sign}(\omega_{ni}) \times q}^2 \quad (8)$$

In these formula,  $q$  gives the laser polarization ( $q = -1, 0, +1$ ), and the 3J coefficient  $C_{J_i, M_{J_i}, J_n, q}$  is equal to

$$\begin{pmatrix} J_i & 1 & J_n \\ -M_{J_i} & -q & M_{J_i} + q \end{pmatrix}.$$

The light shift can therefore be written to the lowest order in perturbation theory as [18]:

$$U_{i, M_{J_i}}(r) = -3\pi c^2 I_L(r) \sum_n \frac{\text{sign}(\omega_{ni}) \gamma_{M_{J_i}, n}}{\omega_{ni}^2 (\omega_{ni}^2 - \omega^2)} \quad (9)$$

Some simplification occurs if the state  $i$  and all the states it is coupled to belong to true spectroscopic terms, which means that they are fully characterized by their total orbital momentum,  $L$ , and spin,  $S$ , in addition to their total momentum  $J$ . First, the cycling rate  $\gamma_{ni}$  does not depend on the fine structure. Then, if the laser frequency is red detuned enough so that all the detunings are large compared to the fine structure splitting, we can use the following sum rule over the 3J coefficients for further simplification:

$$\sum_{J_n = J_{i-1}, J_i, J_{i+1}} (2 \times J_n + 1) C_{J_i, M_{J_i}, J_n, q}^2 = 1, \forall q \quad (10)$$

Finally, if the state  $i$  is only coupled to more energetic states, the light shifts depend neither on  $M_{J_i}$ , nor on the laser polarization. This explains why the fine structure can be ignored when evaluating the light shift of the ground state in various instances.

However, this simplification is not valid anymore if either the state  $i$  or the levels it is coupled to, are not pure spectroscopic terms (which is the case when  $\gamma_{ni}$  depend on  $J_n$ ). This is indeed the case for Chromium. The coupling of the ground state  ${}^7S_3$  to excited  $P$  states depends on the fine structure of these excited states. The effect is even larger for the  ${}^5D$  metastable states, which are themselves not pure spectroscopic terms (as clearly shown by their non zero coupling to the  ${}^7P$  state).

To evaluate the light shifts of the levels of interest at the center of the IR laser beam from eq. (9), we used the spectroscopic data available from NIST [19] for the

atomic level energies and the coupling rates, and we took for  $I_L(r)$  the experimental laser intensity peak given by the measurements of the laser power ( $P=29$  W) and waist ( $W=55$   $\mu\text{m}$ ):  $I_L = 2 \times P/(\pi W^2)$ . Because the parametric excitation is performed in the mixed trap where the magnetic field direction is not constant, there is no good choice for  $q$ . As the laser polarization is linear, the polarizations seen by the atoms in the mixed trap change between a  $\pi$  polarization ( $q = 0$ ), and an equal mix  $-\sigma_{inc}$  polarization of  $\sigma+$  ( $q = 1$ ) and  $\sigma-$  ( $q = -1$ ) polarizations, corresponding to a local B field respectively orthogonal and parallel to the laser propagation axis. We give below (in MHz) the results obtained for both states:

$$\begin{aligned} U_{0^7S_3,M} &=_{\sigma_{inc}} -2.525 - 0.004 \times M^2 \\ &=_{\pi} -2.574 + 0.008 \times M^2 \\ U_{0^5D_4,M} &=_{\sigma_{inc}} -1.925 - 0.015 \times M^2 \\ &=_{\pi} -2.220 + 0.03 \times M^2 \end{aligned} \quad (11)$$

For both polarizations, the quadratic dependance on  $M$  is a result of properties of the 3J coefficients [20].

As discussed above, there are small differences for the light shifts of the ground state Zeeman sublevels, with a maximum of the order of 3%. We want to stress that this energy splitting has to be taken into account when evaluating spinor BEC phase diagrams [21] in an OT. Nevertheless, the fact that these energy shifts remain small in percentage allows us to compare the theoretical results and the experimental one.

The situation is quite different for the  $^5D_4$  level: up to 21% differences are expected between the light shifts of the  $M_J = 4$  and  $M_J = 0$  sublevels for a  $\pi$  polarization. Therefore, an accurate comparison between theory and experience would require to work with a polarized atomic sample, but we cannot achieve this polarization experimentally, as any experimentally accessible optical excitation from the  $D$  metastable states drives the atoms to other levels. Besides, it should be noted that spectroscopic data concerning the couplings of the metastable state are less complete than the ones of the ground state.

We see that the theoretical values of eq. (11) are below our experimental light shifts measurements for both the  $^7S_3$  and the  $^5D_4$  state, although within the error bars. We are still investigating this issue. One possibility is that the IR laser mode at the atoms location is affected by systematic thermal effects induced by the crossing of the viewports of the experimental chamber.

In conclusion, we have optically trapped metastable Cr atoms, using a new accumulation procedure. We have identified the leading loss mechanism which limits the accumulation of atoms. The trap characterization shows that we have obtained a promising starting point to reach Cr quantum degeneracy following a new strategy. The measurement of the trap depth is in reasonable agreement with calculations based on available spectroscopic data. For atoms having a complicated electronic structure such as Cr, our calculations stress the absence of energy degeneracy among the different subZeeman states in an OT, even if it is created by a far red detuned laser.

## References

1. M.D. Barrett et al., Phys. Rev. Lett., **87**, 010404 (2001)
2. T. Weber et al., Science **299**, 232 (2003)
3. A. Griesmaier et al., Phys. Rev. Lett., **94** 160401 (2005)
4. D. Guéry-Odelin et al., Europhys. Lett., **44**, 25 (1998)
5. Y. Takasu et al., Phys. Rev. Lett., **91** 040404 (2003)
6. C. C. Bradley et al., Phys. Rev. A, **61**, 053407 (2000)
7. R. Chicireanu et al., Phys. Rev. A, **73**, 053406 (2006)
8. M. Baranov et al., Phys. Scr. T102, 74 (2002)
9. J. Stuhler et al., Phys. Rev. A, **64**, 031405R (2001)
10. A. Griesmaier et al, Appl. Phys. B, **82**, 211 (2006)
11. R. Chicireanu et al., submitted (arxiv.org/physics/0612133)
12. K.M. O'Hara et al., Phys. Rev. A, **63**, 043403 (2001)
13. S.J.M. Kuppens et al., Phys. Rev. A, **62**, 013406 (2000)
14. W. Petrich et al., Phys. Rev. Lett., **74**, 3352 (1995)
15. S. Friebe et al., Phys. Rev. A, **57**, R20-R23 (1998)
16. K.M. O'Hara, Optical Trapping and Evaporative cooling of Fermionic Atoms, Ph.D thesis (Subsection 7.5), Duke University (2000)
17. A. Griesmaier, Dipole-dipole interaction in a degenerate quantum gas, Ph.D thesis (Subsection 4.6), Stuttgart University (2006)
18. R. Grimm, M. Weidemüller, and Yu.B. Ovchinnikov, Adv. At. Mol. Opt. Phys., **42**, 95 (2000)
19. <http://physics.nist.gov/PhysRefData/ASD/index.html>
20.  $C_{J_i, M_{J_i}, J_n, 0}^2$ , or the sum ( $C_{J_i, M_{J_i}, J_n, 1}^2 + C_{J_i, M_{J_i}, J_n, -1}^2$ ), do not include any term proportionnal to  $M_{J_i}$ , for  $J_n = J_{i-1}, J_i, J_{i+1}$ .
21. See for example C.K. Law et al., Phys. Rev. Lett., **81** 5257 (1998), L. Santos and T. Pfau, Phys. Rev. Lett., **96** 190404 (2006)